



## Supplementary materials for

Mai TANG, Wenqiang XIA, Jiuqiang DENG, Yao MAO, 2025. An error-based observer improved by the repetitive control strategy for electro-optical tracking systems. *Front Inform Technol Electron Eng*, 26(3):441-455.  
<https://doi.org/10.1631/FITEE.2300796>

### Proof of Theorem 1

After sorting out the tracking transfer function formula, it can be easily known that the numerator polynomial of TTF and the characteristic polynomial of RCEOB are

$$\begin{aligned}
 \text{num}_{\text{TTF}} &= C_{\text{RC}}(s)G(s) + G(s)G^{-1}(s)Q(s) \\
 &= \frac{C(s)G(s) + G(s)G^{-1}(s)Q(s)(1 - e^{-T_{\text{P}}s}q(s))}{1 - e^{-T_{\text{P}}s}q(s)}, \\
 P(s) &= 1 + C_{\text{RC}}(s)G(s) + Q(s)(G(s)G^{-1}(s) - 1) \\
 &= \frac{C(s)G(s) + (1 - e^{-T_{\text{P}}s}q(s))[Q(s)(G(s)G^{-1}(s) - 1) + 1]}{1 - e^{-T_{\text{P}}s}q(s)}.
 \end{aligned} \tag{S1}$$

Then the TTF of RCEOB can be simplified as follows:

$$\begin{aligned}
 \text{TTF}_{\text{RCEOB}} &= \frac{\text{num}_{\text{TTF}}}{P(s)} \\
 &= \frac{C(s)G(s) \left[ 1 + \frac{G^{-1}(s)Q(s)(1 - e^{-T_{\text{P}}s}q(s))}{C(s)} \right]}{(1 + C(s)G(s)) \left\{ 1 + \frac{(1 - e^{-T_{\text{P}}s}q(s))[Q(s)(G(s)G^{-1}(s) - 1) + 1] - 1}{1 - e^{-T_{\text{P}}s}q(s)} \right\}} \\
 &= \frac{C(s)G(s)}{1 + C(s)G(s)} \frac{1}{1 + \frac{e^{-T_{\text{P}}s}q(s)C(s) - (1 - e^{-T_{\text{P}}s}q(s))(C(s)Q(s) + G^{-1}(s)Q(s))}{(1 + C(s)G(s))[C(s) + G^{-1}(s)Q(s)(1 - e^{-T_{\text{P}}s}q(s))]}}.
 \end{aligned} \tag{S2}$$

According to Eq. (S1),  $1 + C(s)G(s)$  is the characteristic polynomial of the transfer function of the system in a single closed loop, and the experimental results of the single closed loop ensure that  $C(s)$  is stable, so the solution of  $1 + C(s)G(s) = 0$  must be on the left side of the negative half plane in the complex domain. Therefore, to ensure the stability of the RCEOB system under the multi-filter structure, it is necessary to ensure that the other multiplying factor besides  $1 + C(s)G(s)$  in Eq. (S2) satisfies the stability condition. According to the small gain theorem (Teel, 1996), the following conditions can be obtained:

$$\left\| \frac{e^{-T_{\text{P}}s}q(s)C(s) - (1 - e^{-T_{\text{P}}s}q(s))(C(s)Q(s) + G^{-1}(s)Q(s))}{(1 + C(s)G(s))[C(s) + G^{-1}(s)Q(s)(1 - e^{-T_{\text{P}}s}q(s))]} \right\|_{\infty} < 1. \tag{S3}$$

The above equation is the stability condition given in Theorem 1.

## Proof of Theorem 2

The simplified transfer function formula can be obtained from the analysis of Eq. (3):

$$\begin{aligned}
\text{TTF}_{\text{RCEOB}} &= \frac{Y(s)}{R(s)} \\
&= \frac{C_{\text{RC}}(s)G(s) + G(s)G^{-1}(s)Q(s)}{1 + C_{\text{RC}}(s)G(s) + G(s)G^{-1}(s)Q(s) - Q(s)} \\
&= \frac{C(s)G(s) + G(s)G^{-1}(s)Q(s)(1 - e^{-T_{\text{P}}s}q(s))}{P(s)(1 - e^{-T_{\text{P}}s}q(s))}.
\end{aligned} \tag{S4}$$

Considering the uncertainty of the model on the basis of the closed-loop transfer function of the control system, the updated characteristic polynomial can be obtained as follows:

$$\begin{aligned}
P_{\text{P}}(s) &= C(s)G_{\text{P}}(s)(1 - e^{-T_{\text{P}}s}q(s)) \\
&+ Q(s)(G_{\text{P}}(s)G^{-1}(s))(1 - e^{-T_{\text{P}}s}q(s))^2 \\
&= C(s)G(s)(1 + \Delta(s))(1 - e^{-T_{\text{P}}s}q(s)) \\
&+ Q(s)[G(s)(1 + \Delta(s))G^{-1}(s)](1 - e^{-T_{\text{P}}s}q(s))^2 \\
&= [C(s)G(s) + Q(s)(G(s)G^{-1}(s))(1 - e^{-T_{\text{P}}s}q(s))] \\
&\cdot (1 + \Delta(s)\text{TTF}_{\text{RCEOB}}(s))(1 - e^{-T_{\text{P}}s}q(s)) \\
&= P(s)(1 + \Delta(s)\text{TTF}_{\text{RCEOB}}(s)).
\end{aligned} \tag{S5}$$

In Eq. (S5),  $P(s)$  and  $\text{TTF}_{\text{RCEOB}}(s)$  are given by the characteristic polynomial and the tracking transfer function, respectively. On the premise that Theorem 1 is satisfied,  $P(s)$  satisfies the stability condition. To ensure the robust stability of the RCEOB system, according to the small gain theorem, conditions need to be satisfied as follows:  $\|\Delta(s)\text{TTF}_{\text{RCEOB}}(s)\|_{\infty} < 1$ .

## Proof of Theorem 3

$Q_{\text{N}}(s)$ 's complementary sensitivity function can be expressed as

$$\begin{aligned}
\text{ESF}_{Q_{\text{N}1}} &= 1 - Q_{\text{N}}(s) \\
&= \frac{s^2 + \eta_1\omega_1s + \omega_1^2}{s^2 + \alpha_1\eta_1\omega_1s + \omega_1^2} \cdot (1 - q_{\text{LPP}}(s)) \\
&= \frac{s^2 + \eta_1\omega_1s + \omega_1^2}{s^2 + \alpha_1\eta_1\omega_1s + \omega_1^2} \cdot \frac{Ts}{Ts + 1}.
\end{aligned} \tag{S6}$$

To understand the performance at a specific frequency, first derive the amplitude response of the complementary sensitivity function:

$$\begin{aligned}
|\text{ESF}_{Q_{\text{N}1}}(j\omega)|^2 &= \text{ESF}_{Q_{\text{N}1}}(j\omega) \cdot \text{ESF}_{Q_{\text{N}1}}(-j\omega) \\
&= \frac{\omega_1^2 - \omega^2 + \eta_1\omega_1j\omega}{\omega_1^2 - \omega^2 + \alpha_1\eta_1\omega_1j\omega} \cdot \frac{\omega_1^2 - \omega^2 - \eta_1\omega_1j\omega}{\omega_1^2 - \omega^2 - \alpha_1\eta_1\omega_1j\omega} \cdot \frac{Tj\omega}{Tj\omega + 1} \cdot \frac{Tj\omega}{Tj\omega - 1} \\
&= \frac{(\omega_1^2 - \omega^2)^2 + \eta_1^2\omega_1^2\omega^2}{(\omega_1^2 - \omega^2)^2 + \alpha_1^2\eta_1^2\omega_1^2\omega^2} \cdot \frac{T^2\omega^2}{T^2\omega^2 + 1}.
\end{aligned} \tag{S7}$$

Find the partial derivative of the amplitude response with respect to the frequency  $\omega$ :

$$\begin{aligned}
& \frac{\partial |\text{ESF}_{Q_{N1}}(j\omega)|^2}{\partial \omega} \\
&= \frac{[2(\omega_1^2 - \omega^2)(1 - 2\omega) + 2\eta_1^2 \omega_1^2 \omega] T^2 \omega^2}{[(\omega_1^2 - \omega^2)^2 + \alpha_1^2 \eta_1^2 \omega_1^2 \omega^2] (T^2 \omega^2 + 1)} \\
&+ \frac{[(\omega_1^2 - \omega^2)^2 + \eta_1^2 \omega_1^2 \omega^2] 2T^2 \omega}{[(\omega_1^2 - \omega^2)^2 + \alpha_1^2 \eta_1^2 \omega_1^2 \omega^2] (T^2 \omega^2 + 1)} \\
&- \left\{ \frac{[2(\omega_1^2 - \omega^2)(1 - 2\omega) + 2\alpha_1^2 \eta_1^2 \omega_1^2 \omega] T^2 \omega^2}{[(\omega_1^2 - \omega^2)^2 + \alpha_1^2 \eta_1^2 \omega_1^2 \omega^2] (T^2 \omega^2 + 1)} \right. \\
&+ \left. \frac{[(\omega_1^2 - \omega^2)^2 + \alpha_1^2 \eta_1^2 \omega_1^2 \omega^2] 2T^4 \omega^3}{[(\omega_1^2 - \omega^2)^2 + \alpha_1^2 \eta_1^2 \omega_1^2 \omega^2] (T^2 \omega^2 + 1)^2} \right\} \\
&\cdot \frac{[(\omega_1^2 - \omega^2)^2 + \eta_1^2 \omega_1^2 \omega^2]}{[(\omega_1^2 - \omega^2)^2 + \alpha_1^2 \eta_1^2 \omega_1^2 \omega^2] (T^2 \omega^2 + 1)^2}.
\end{aligned} \tag{S8}$$

The above equation can be rearranged to obtain the following expression:

$$\begin{aligned}
& \frac{\partial |\text{ESF}_{Q_{N1}}(j\omega)|^2}{\partial \omega} \\
&= \frac{(1 - \alpha_1^2) T^2 (\omega^8 \omega_1^2 - \omega^4 \omega_1^6) + (6 + \alpha_1^2 \eta_1^4 - 2\alpha_1^2 \eta_1^2 - 2\eta_1^2) \omega^4 \omega_1^4}{[(\omega_1^2 - \omega^2)^2 + \alpha_1^2 \eta_1^2 \omega_1^2 \omega^2]^2 (T^2 \omega^2 + 1)^2} \\
&+ \frac{(2\eta_1^2 - 4) \omega^2 \omega_1^6 + (2\alpha_1^2 \eta_1^2 - 4) \omega^6 \omega_1^2 + \omega^8 + \omega_1^8}{[(\omega_1^2 - \omega^2)^2 + \alpha_1^2 \eta_1^2 \omega_1^2 \omega^2]^2 (T^2 \omega^2 + 1)^2}.
\end{aligned} \tag{S9}$$

When  $\omega \ll \omega_1, \omega \rightarrow 0$ , it is not difficult to see from Eq. (S9) that at this time  $\frac{\partial |\text{ESF}_{Q_{N1}}(j\omega)|^2}{\partial \omega} \approx 1 > 0$ . When  $\omega = \omega_1$ ,  $\frac{\partial |\text{ESF}_{Q_{N1}}(j\omega)|^2}{\partial \omega} = 0$ , which means that the amplitude response must cross zero; thus, there is an extreme value at  $\omega = \omega_1$ . Combined with the variation of factors in the frequency response formula, we can see that the amplitude response function increases monotonically at first, reaches a maximum value between  $0 \sim \omega_1$ , and reaches a minimum value when  $\omega = \omega_1$ .

## Proof of Theorem 4

When  $a \neq 1$ , the complementary sensitivity function is

$$\begin{aligned}
& \text{ESF}_{Q_{Nn}} = 1 - Q_N(s) \\
&= \prod_{i=1}^a \frac{s^2 + \eta_i \omega_i s + \omega_i^2}{s^2 + \alpha_i \eta_i \omega_i s + \omega_i^2} \cdot (1 - q_{\text{LPF}}(s)) \\
&= \prod_{i=1}^a \frac{s^2 + \eta_i \omega_i s + \omega_i^2}{s^2 + \alpha_i \eta_i \omega_i s + \omega_i^2} \cdot \frac{Ts}{Ts + 1}.
\end{aligned} \tag{S10}$$

Also, analyze the amplitude response:

$$\begin{aligned}
|\text{ESF}_{Q_{Nn}}(j\omega)|^2 &= \text{ESF}_{Q_{Nn}}(j\omega) \cdot \text{ESF}_{Q_{Nn}}(-j\omega) \\
&= \prod_{i=1}^a \frac{\omega_i^2 - \omega^2 + \eta_i \omega_i j\omega}{\omega_i^2 - \omega^2 + \alpha_i \eta_i \omega_i j\omega} \cdot \frac{\omega_i^2 - \omega^2 - \eta_i \omega_i j\omega}{\omega_i^2 - \omega^2 - \alpha_i \eta_i \omega_i j\omega} \cdot \frac{Tj\omega}{Tj\omega + 1} \cdot \frac{Tj\omega}{Tj\omega - 1} \\
&= \prod_{i=1}^a \frac{(\omega_i^2 - \omega^2)^2 + \eta_i^2 \omega_i^2 \omega^2}{(\omega_i^2 - \omega^2)^2 + \alpha_i^2 \eta_i^2 \omega_i^2 \omega^2} \cdot \frac{T^2 \omega^2}{T^2 \omega^2 + 1}.
\end{aligned} \tag{S11}$$

Before obtaining the partial derivative, combining the difference between Eqs. (8) and (S9), and analyzing the amplitude response of Eqs. (S6) and (S8) for  $a \neq 1$ , it is not difficult to see that the main change of amplitude response is the increase of multiplicative structure when compared with  $k = 1$ . According to the chain derivation rule, after obtaining the partial derivative, the analysis of the minimum point leads to the following conclusions: before the first trapping point  $\omega_1$ , when  $\omega \ll \omega_1, \omega \rightarrow 0$ , then  $\frac{\partial |\text{ESF}_{Q_{Nn}}(j\omega)|^2}{\partial \omega} \approx 1 > 0$ ; between different trapping points, there is always  $\frac{\partial |\text{ESF}_{Q_{Nn}}(j\omega)|^2}{\partial \omega} \approx 1 > 0$ ; when  $\omega = \omega_i, i \in [1, k]$ , there is always  $\frac{\partial |\text{ESF}_{Q_{Nn}}(j\omega)|^2}{\partial \omega} = 0$ .

## Proof of Theorem 5

The improved repetitive controller structure can be obtained:

$$\begin{aligned}
C_{\text{RC}} &= \frac{C(s)}{1 - e^{-T_P s} q_{\text{new}}(s)} \\
&= \frac{C(s) [1 - (1 - k)e^{-T_P s}]}{1 - ke^{-T_P s} q(s)}.
\end{aligned} \tag{S12}$$

It is assumed that when  $k = 1$ , it is analyzed as an ideal case, and the filter structure has changed at this time. In the process of gradually reducing the value of  $k$ , the total gain of the controller  $1 - (1 - k)e^{-T_P s}$  gradually decreases under the condition that the  $C(s)$  structure remains unchanged. At the same time,  $1 - ke^{-T_P s}$  can still provide the notch effect at the set frequency within the value range of  $k \neq 0$ , thus realizing the signal amplification problem at the non-notch frequency.

## Closed-loop experimental result analysis

Among them, Single Loop is the single closed-loop experimental result when  $C(s)$  is the controller, EOB is the experimental result when only EOB structure exists, RC is the experimental result when only repetitive controller exists, RCEOB is the experimental result when  $Q(s)$  is the low-pass filter in the composite control structure, and the last two are the composite control improved scheme of different filters in the structure.

In the curve of the disturbance suppression function, the smaller the value of the function at a specific frequency point is, the better the disturbance suppression performance of the control structure at the corresponding frequency is proved. Based on this analysis of the experimental results shown in Fig. 19, it can be easily seen that RCEOB does have significant improvement in disturbance suppression performance.

The composite controller containing  $Q_N(s)$  can effectively realize notch beyond the repetitive controller's periodic harmonic frequency points, including  $Q_{\text{RC}}(s)$ . The structure of the composite controller achieves the double-notch structure at the set frequencies of 1 Hz and 5 Hz simultaneously.

Table S1 is a comparison of the performance improvement of the composite controller structure containing  $Q_N(s)$  at 2 Hz and 5 Hz. The definition of the performance index is the increase of the magnitude of the notch point.

Through comparison, it can be seen that the performance of the composite structure at 2 Hz and 5 Hz is intuitively improved. Because 5 Hz is the harmonic frequency notch brought by the repetitive controller,

**Table S1 Performance comparison of closed-loop test results at specific frequency points**

Method	Error tracking		Disturbance suppression	
	2 Hz	5 Hz	2 Hz	5 Hz
Single Loop	107.7%	833.3%	70.0%	733.3%
RC	125.0%	3.7%	78.9%	8.69%
EOB	40.0%	460.0%	30.8%	525.0%

its effect is better than that of the discrete frequency notch brought by the inclusion of  $Q_N(s)$ , but the latter can be flexibly adjusted according to different actual conditions, and the flexibility of parameter selection is better than the former. At the same time, it can be seen that the improvement of the filter in EOB has a certain effect on the notch of the harmonic frequency doubling set by the repetitive controller.

### Experimental results of single-frequency disturbance

To verify the notch effect at the set frequency, we need to clarify how to achieve the suppression of periodic disturbance. Let the whole system be a closed loop and have a stable situation, add different frequencies of periodic disturbance, and observe the relationship between disturbance input and system output: the following compares the changes in the time domain of the system output after the periodic disturbances of frequencies of 1, 2, 4, and 5 Hz is added to the single closed loop and RCEOB with  $Q_N(s)$ , respectively, when the system is stabilized. The sampling frequency of the system is 100 Hz.

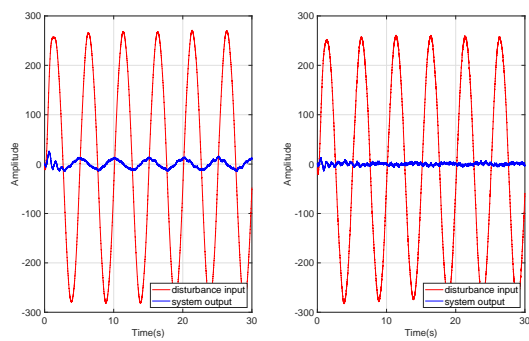
After the most intuitive analysis of the experimental results, it can be easily seen that the RCEOB structure has better disturbance suppression performance than the single closed loop in each group of controlled experiments, and the system output can be re-stabilized and controlled within a small range in a very short time, and the improvement of the disturbance suppression ability of RCEOB at various frequencies can be seen obviously. At the same time, comparing the experimental results at 4 Hz and 5 Hz, it can be seen that RCEOB has significantly better suppression ability for periodic disturbance signals at 5 Hz than at 4 Hz, achieving the trapping effect foreseen in parameter design, and also reflecting that the composite controller has better disturbance suppression ability at the set frequency.

### Experimental results of multi-frequency disturbance

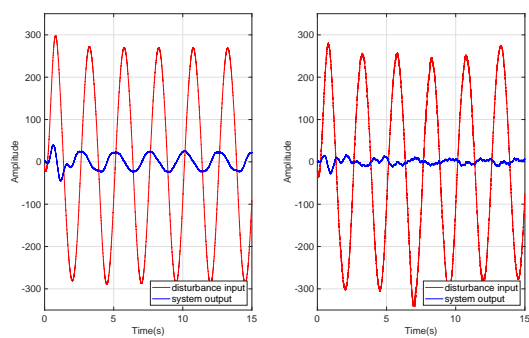
To further verify that the composite controller can cope with the disturbance in the case of complex disturbance, the realization of multiple notches is demonstrated in the experiment process, and it is proved that both  $Q_N(s)$  and  $Q_{RC}(s)$  can realize multiple notches. Two periodic disturbances of different frequencies are selected to act on the system at the same time. By directly enhancing the complexity of the disturbances, the output of the system after stabilization under different methods is observed, and the output of the system under different combinations of periodic disturbances is compared.

Comparing the single closed-loop system in Fig. S1, it can be seen that the influence of multi-period disturbance input in the composite control system of the two structures is significantly smaller than that in the single closed-loop system under the condition of single period disturbance input. This directly shows that the composite controller structure can realize the suppression of complex disturbance at multi-frequency points.

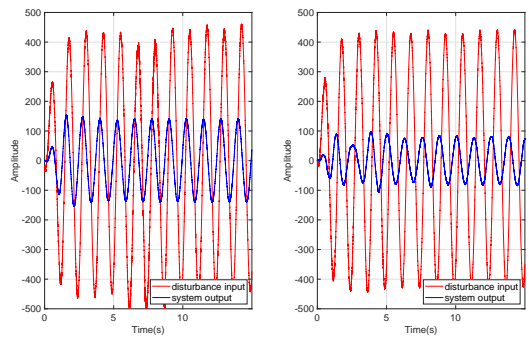
At the same time, it can be seen from the experimental results given in Fig. S2 that the composite control system can still suppress the disturbance when the amplitude increases significantly, so that the system output can be kept within an acceptable range. The above experiments validate the effectiveness of composite controller structure RCEOB through the parameter design given in the theoretical analysis, and different filter structures are implemented, showing that the multiple notch structure given in the theoretical analysis is feasible. On this basis, the operating performances of the system under different disturbance conditions are compared, and it is concluded that RCEOB does improve the disturbance suppression ability



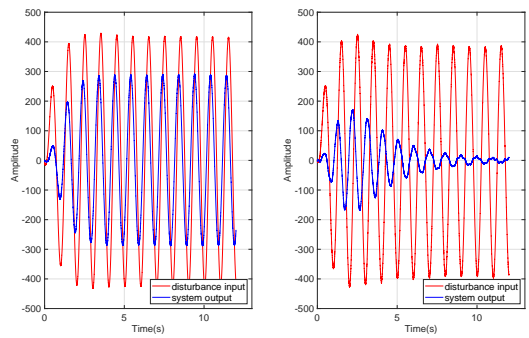
(a)



(b)

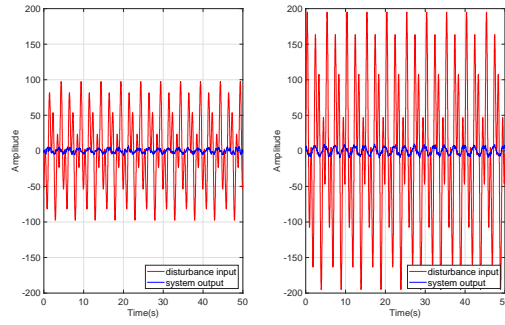


(c)

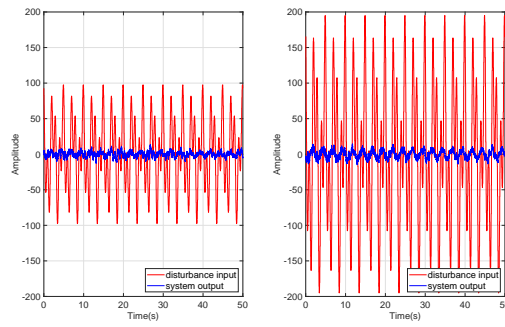


(d)

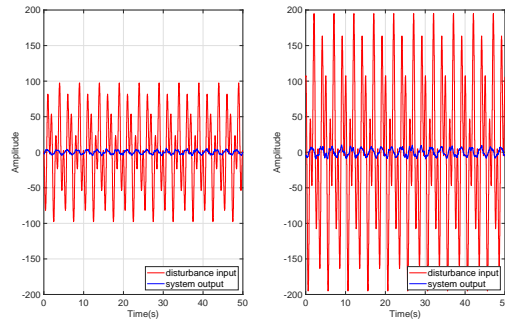
**Fig. S1 Comparison of system output under disturbance input of 1 Hz (a), 2 Hz (b), 4 Hz (c), and 5 Hz (d). Left: single closed loop; right: RCEOB**



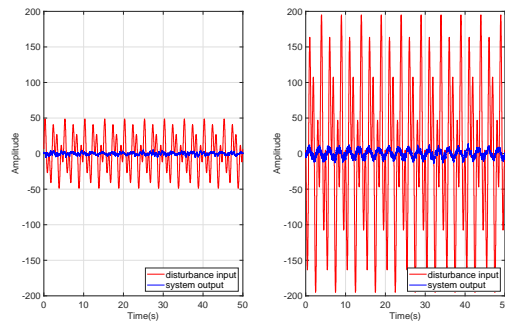
(a)



(b)



(c)



(d)

Fig. S2 System output of two composite structures under complex disturbance: (a) RCEOB with  $Q_N$  at 2 Hz+5 Hz with an amplitude of 50 (left) and 100 (right); (b) RCEOB with  $Q_N$  at 5 Hz+10 Hz with an amplitude of 50 (left) and 100 (right); (c) RCEOB with  $Q_{RC}$  at 2 Hz+5 Hz with an amplitude of 50 (left) and 100 (right); (d) RCEOB with  $Q_{RC}$  at 5 Hz+10 Hz with an amplitude of 50 (left) and 100 (right)

of the system, which proves that the control method proposed in this work can improve the operating performance of the electro-optical system under multi-period and discrete point disturbance conditions.

### **Reference**

Teel AR, 1996. A nonlinear small gain theorem for the analysis of control systems with saturation. *IEEE Trans Automat Contr*, **41**(9):1256-1270.